



## Research article

# CD133<sup>+</sup>/ABCC5<sup>+</sup> cervical cancer cells exhibit cancer stem cell properties

Lin He<sup>a</sup>, Hengjun Qian<sup>b</sup>, Ayinuer seyiti<sup>c</sup>, Chengshaoxiong Yang<sup>a</sup>, Ning Shi<sup>a</sup>,  
Chen Chen<sup>a</sup>, Pingxu Zhang<sup>a</sup>, Youxiang Hou<sup>c,\*</sup>

<sup>a</sup> Tumor Hospital Affiliated to Xinjiang Medical University, Urumqi, Xinjiang, 830011, PR China

<sup>b</sup> Yibin Second People's Hospital, Sichuan, 644002, PR China

<sup>c</sup> Department of Radiation Oncology, The Affiliated Cancer Hospital of Xinjiang Medical University, Xinjiang, 830011, PR China

## ARTICLE INFO

## Keywords:

FOXMI

ABCC5

Cervical cancer

Paclitaxel

## ABSTRACT

**Objective:** This study explores the correlation between Forkhead box M1 (FOXMI) and ATP-binding cassette subfamily C member 5 (ABCC5) in relation to paclitaxel resistance in cervical cancer. It aims to identify potential cervical cancer stem cell markers, offering fresh perspectives for developing therapeutic strategies to overcome paclitaxel chemoresistance in cervical cancer. **Methods:** Paclitaxel-resistant Hela cells (Hela/Taxol) were developed by intermittently exposing Hela cells to progressively increasing concentrations of paclitaxel. We assessed the biological properties of both Hela and Hela/Taxol cells using various assays: cell proliferation, clonogenic, cell cycle, apoptosis, scratch, and transwell. To determine which markers better represent tumor stem cells, we analyzed various known and potential stem cell markers in combination. Flow cytometry was employed to measure the proportion of positive markers in both parental and drug-resistant cell lines. Following statistical analysis to establish relative stability, CD133+ABCC5+ cells were sorted for further examination. Subsequent tests included sphere-forming assays and Western blot analysis to detect the presence of the stem cell-specific protein Sox2, aiding in the identification of viable cervical cancer stem cell markers.

**Results:** The Hela/Taxol cell line exhibited significantly enhanced proliferation, migration, and invasion capabilities compared to the Hela cell line, alongside a marked reduction in apoptosis rates ( $P < 0.01$ ). Notably, proportions of CD44<sup>+</sup>, CD24<sup>+</sup>CD44<sup>+</sup>, ABCC5<sup>+</sup>, CD24<sup>+</sup>CD44<sup>+</sup>ABCC5<sup>+</sup>, CD44<sup>+</sup>ABCC5<sup>+</sup>, CD24<sup>+</sup>CD44<sup>+</sup>FOXMI<sup>+</sup>, CD44<sup>+</sup>FOXMI<sup>+</sup>, CD133+ABCC5<sup>+</sup>, and CD133+FOXMI<sup>+</sup> were significantly higher ( $P < 0.05$ ). Furthermore, the size and number of spheres formed by CD133+ABCC5+ cells were greater in the sorted Hela/Taxol line ( $P < 0.01$ ), with increased expression of the stem cell marker Sox2 ( $P < 0.001$ ).

**Conclusion:** The Hela/Taxol cells demonstrate increased tumoral stemness, suggesting that CD133+ABCC5+ may serve as a novel marker for cervical cancer stem cells.

## 1. Introduction

Globally, cervical cancer ranks as the fourth most prevalent cancer among women, following breast, colorectal, and lung cancers.

\* Corresponding author. Department of Radiation Oncology, The Affiliated Cancer Hospital of Xinjiang Medical University, 789 Suzhou Dong Jie, Xinshi District, Urumqi, Xinjiang, 830011, PR China.

E-mail address: [houyouxiang119@sohu.com](mailto:houyouxiang119@sohu.com) (Y. Hou).

<https://doi.org/10.1016/j.heliyon.2024.e37066>

Received 24 May 2024; Received in revised form 22 August 2024; Accepted 27 August 2024

Available online 29 August 2024

2405-8440/© 2024 The Authors. Published by Elsevier Ltd. This is an open access article under the CC BY-NC license (<http://creativecommons.org/licenses/by-nc/4.0/>).

Annually, it accounts for approximately 600,000 new cases and 340,000 deaths, with about 83 % of new cases and 88 % of deaths occurring in low-income countries [1–3]. In China, the incidence rate of cervical cancer is 47.8 per 100,000 women, making it the second most common female malignancy after breast cancer. It accounts for 28.8 % of the global new cases annually, with 131,500 new cases reported each year. Recent trends indicate a shift towards younger ages at diagnosis [4,5]. Surgery remains the primary treatment for early-stage cervical cancer, whereas chemotherapy and radiotherapy are crucial for managing advanced stages.

Paclitaxel, a tetracyclic diterpenoid secondary metabolite originally isolated from the bark of the Pacific yew, is now predominantly derived from plants in the genus *Picea*. It is acknowledged globally as one of the most effective anticancer agents, demonstrating significant efficacy against various cancers including ovarian, breast, lung, Kaposi's sarcoma, cervical, and pancreatic cancers [6]. As a common chemotherapeutic agent for cervical cancer, Paclitaxel (PTX) stabilizes microtubules and induces apoptosis by hindering cell mitosis [7].

However, the development of acquired resistance to paclitaxel significantly hampers its clinical efficacy. In the treatment of cervical cancer, chemotherapy regimens consisting of paclitaxel alone or in combination with cisplatin are well-established [8,9]. Despite its efficacy, resistance to paclitaxel frequently emerges with long-term use [10,11]. Therefore, understanding and mitigating drug resistance is essential for enhancing the clinical outcomes and prognosis of cancer patients.

Recent studies suggest that chemotherapy resistance is closely linked to tumor stem cells, which are believed to be a primary reason for the poor outcomes in malignant tumors [12,13]. Tumor stem cells are a subpopulation of cells with biological properties such as self-renewal, multidirectional differentiation, unlimited proliferation, and extreme tumorigenicity. These cells exhibit 3 characteristics, namely self-renewal, pluripotency, and stem cell marker expression [14].

Due to their unique cell biological properties, tumor stem cell theory suggests that tumor invasion and metastasis are closely related to tumor stem cells, and that stem cells may be the intrinsic cause of malignant tumor invasion and metastasis [15]. Tumor stem cells, characterized by self-renewal, multidirectional differentiation, unlimited proliferation, and pronounced tumorigenicity, are also known for their resistance to radiotherapy and their role in promoting metastasis and recurrence, contributing to clinical failures and patient mortality [16]. These cells have been identified in various solid tumors, including cervical cancer, although comprehensive data on cervical cancer stem cells (CSCs) and their impact on disease outcomes remain scarce [17]. Currently, specific markers for cervical cancer stem cells are not well-defined [18].

Preliminary research by our group indicated that paclitaxel resistance in cervical cancer may be linked to decreased intracellular concentrations of the drug, influenced by FOXM1 (Forkhead box protein M1) and its modulation of ABCC5 (ATP-binding cassette transporter protein C5) [19]. This interaction also appears to enhance the characteristics of paclitaxel-resistant cervical cancer stem cells [20]. Given the significant roles of FOXM1 and ABCC5 in cancer progression and stem cell properties [21–24], their potential as markers for tumor stem cells merits further exploration. This study aims to delve deeper into the relationship between cervical cancer stem cells and paclitaxel resistance, potentially providing a theoretical foundation for identifying new therapeutic targets to combat resistance in cervical cancer cells.

## 2. Materials and methods

### 2.1. Clone formation assay

Hela cells were sourced from Bei-Na Biotech, and Hela paclitaxel-resistant cell lines (Hela/Taxol cells) were obtained from Tong-Pai Biotech. Both cell types in logarithmic growth phase were cultured in RPMI-1640 medium supplemented with 10 % FBS, 100 U/ml penicillin, and 100 µg/ml streptomycin, and incubated at 37 °C in a 5 % CO<sub>2</sub> atmosphere. After counting, cells were diluted to a concentration of  $2 \times 10^4$  cells/ml. Each well of a six-well plate was seeded with 2000 cells in 2 ml of medium, and the plate was shaken using the cross method to ensure uniform cell distribution. Following overnight incubation for cell attachment, the medium was replaced with 2 ml of paclitaxel-containing medium at the designated concentration. Cultivation continued for 2–3 weeks until visible colonies formed. Colonies were then fixed with methanol for 1 h after discarding the old medium and washing twice with PBS. Fixed cells were stained with 0.1 % crystal violet for 1 h, washed with PBS, dried, and imaged for colony counting.

### 2.2. MTT assay

Hela and Hela/Taxol cells were seeded at  $5 \times 10^3$  cells/well in 96-well plates and cultured overnight. Cells were treated with various concentrations of paclitaxel (0.01, 0.1, 1, 10, 50, and 100 µM, supplied by Mylan Bio Inc.). At 24 and 48 h post-treatment, 20 µl of MTT solution (Promega) was added to each well, followed by a 4 h incubation at 37 °C in 5 % CO<sub>2</sub>. Subsequently, 100 µl of solubilization solution was added to dissolve the formazan crystals. Absorbance was measured at 570 nm using a spectrophotometer. Cell viability was calculated using the formula: control optical density (OD-experimental OD)/control OD.

### 2.3. Determination of apoptosis rate (Annexin-V/PI Double Staining Assay)

Hela cells and Hela/Taxol cells were harvested, trypsinized, and washed twice with PBS. Cells ( $5 \times 10^5$ ) were resuspended in 500 µl of Binding Buffer, to which 5 µl each of Annexin-V/FITC and PI staining solutions were added. The mixture was incubated at room temperature, shielded from light, for 15 min. Apoptosis rates were subsequently assessed using a flow cytometer (BD Biosciences).

#### 2.4. Cell scratch assay

Hela and Hela/Taxol cells were seeded at  $5 \times 10^5$  cells/well in 6-well plates and cultured in RPMI-1640 medium supplemented with 10 % FBS (GIBCO Inc.) for 24 h. After reaching confluence, the cell monolayers were scratched with a 200  $\mu$ l pipette tip and washed three times with PBS. The cells were then cultured in RPMI-1640 medium containing 1 % FBS. The gap closure was measured at intervals of 0, 12, 24, and 48 h post-scratch. Cell migration was quantified using the formula: (cell gap at 0 h - cell gap at 12 h/cell gap at 0 h  $\times$  100 %).

#### 2.5. Transwell invasion assay

Hela cells and Hela/Taxol cells were cultured in serum-free RPMI-1640 medium for 48 h prior to the assay. The microporous polycarbonate membranes of transwell chambers (Costar) were coated with Substrate adhesive (Solepol). Each cell ( $5 \times 10^5$ ) type was inoculated into separate upper chambers, and the lower chambers of 24 well plates were filled with RPMI-1640 medium containing 10 % FBS. After a 72 h incubation, the transwells were removed and the cells fixed with 4 % paraformaldehyde for 20 min at room temperature. After washing twice with PBS, 400  $\mu$ l of Giemsa A was added to the wells for 1 min at room temperature, followed by 800  $\mu$ l of Giemsa solution for a reaction of 5 min. Non-migrating cells on the upper membrane were gently removed with a cotton swab. The migrated cells were dried, transferred to slides, and examined under a microscope in three randomly chosen fields to determine the average cell count.

#### 2.6. Flow cytometry sorting of cells

Cell cycle distribution was analyzed using a BD FACSCalibur flow cytometer. Approximately  $1 \times 10^6$  Hela and Hela/Taxol cells were fixed with 5 ml of 70 % ethanol overnight at  $-20^\circ\text{C}$ , protected from light. The following day, the cells were centrifuged at 1000 rpm for 10 min, washed with PBS, and stained with 500  $\mu$ l of PI/RNase staining buffer for 15 min at room temperature in the dark. Cells were then filtered through a 300-mesh screen before analysis with ModFit LT V3.2 software (Mac). For surface staining, CD133-PE, CD44-PE, CD24-PerCP, ABCC5-Alexa Fluor 488, and FOXM1-Alexa Fluor 488 antibodies (Abcam) were added to flow tubes containing Hela and Hela/Taxol cells. Staining analysis was performed using a BD FACSCalibur flow cytometer, and the data analyzed with Diva software. After collection and two PBS washes, cells from adherent cultures of Hela and Hela/Taxol were incubated with PE-labeled mouse anti-human CD133 antibody (BD) and Alexa Fluor 488-labeled secondary antibody for ABCC5 (Invitrogen) at  $37^\circ\text{C}$  for 1 h. After a further two washes with chilled PBS, CD133 and ABCC5 expression was analyzed via flow cytometry using the BD FACSCalibur. Sorting of CD133 and ABCC5 positive cells was conducted using a BD FACSaria flow sorter.

#### 2.7. Stem cell spheroid formation assay

Hela and Hela/Taxol cells were seeded at  $1 \times 10^4$  cells per well in 6 well ultra-low adherence surface culture dishes, with three replicates for each group. The cells were cultured in serum-free DMEM/F12 supplemented with 20  $\mu$ g/L recombinant human epidermal growth factor, 10  $\mu$ g/L human basic fibroblast growth factor, and B27 additives (Mylan Bio). Cell growth and sphere formation were monitored over 10–15 days. Sphere formation rate was calculated using the formula.

#### 2.8. Protein immunoblotting (Western Blot)

Cells were harvested and total protein was extracted using RIPA lysis buffer. Protein samples (30–50  $\mu$ g) were resolved on a 10 % SDS-PAGE gel and transferred onto a PVDF membrane (EMD Millipore). Membranes were blocked using 5 % skim milk powder in TBS-T for 1 h, then incubated overnight at  $4^\circ\text{C}$  with primary antibodies: anti-FOXM1 (1:500; Abcam, ab180710), anti-Sox2 (1:500; Abcam, ab92494), anti-Caspase-3 (1:500; Abcam, ab184787) and anti-Vimentin (1:500; CST, 5741S). After washing thrice with TBS-T, membranes were incubated for 1 h at room temperature with HRP-labeled secondary antibody (1:2000; Santa Cruz Biotechnology, Inc.).

#### 2.9. Statistical analysis

Statistical analyses included the *t*-test and Wilcoxon rank sum test for comparing differences between groups, Spearman rank correlation test for analyzing correlations, and ImageJ for quantitative morphological and protein band analyses. GraphPad Prism 9.0 software was utilized for statistical calculations. Differences were considered statistically significant at a *p*-value of  $<0.05$ .

### 3. Results

#### 3.1. Efficacy of paclitaxel at various concentrations on cell proliferation

By administering varying concentrations of paclitaxel to Hela cells, we observed its impact on cell proliferation. A gradient of five paclitaxel concentrations was used, with each concentration tested in 3–5 replicate wells over a 48 h period. Observations under an inverted microscope showed that higher concentrations of paclitaxel were more effective in inhibiting the proliferation of both Hela

and HeLa/Taxol cells at 24 and 48 h post-treatment, with statistically significant differences noted (Fig. 1A–B,  $P < 0.01$ ). Treatment with IC50 doses of paclitaxel revealed IC50 values for HeLa cells at 4.849  $\mu\text{M}$  after 24 h and 0.568  $\mu\text{M}$  after 48 h (Fig. 1C), while for HeLa/Taxol cells, IC50 values were 47.675  $\mu\text{M}$  after 24 h and 8.070  $\mu\text{M}$  after 48 h (Fig. 1D), indicating significant resistance in HeLa/Taxol cells, with a resistance index of 14.208 (Tables 1–3). Furthermore, clone formation assays demonstrated that HeLa/Taxol cells formed significantly more colonies than HeLa cells, suggesting enhanced proliferative capacity in paclitaxel-resistant cells (Fig. 1D).

### 3.2. Impact of HeLa/Taxol on apoptosis and cell cycle progression

Cell cycle analysis showed that HeLa cells predominantly remained in the G0/G1 phase (Fig. 2A), while HeLa/Taxol cells exhibited a significantly higher proportion in the S phase compared to HeLa cells (Fig. 2B), indicating that HeLa/Taxol cells significantly promoted entry into the DNA synthesis phase (Fig. 2C–Table 4). Apoptosis levels were assessed using Annexin V/PI double staining, revealing significantly lower apoptosis rates in HeLa/Taxol cells compared to HeLa cells (Fig. 2D–E, Table 5), indicating reduced apoptosis in paclitaxel-resistant cells.

### 3.3. Migration and invasion of paclitaxel-resistant HeLa cells

The cell scratch assay demonstrated that the migration rate of HeLa/Taxol cells was significantly higher than that of HeLa cells (Fig. 3A–B). Similarly, results from the trans-well invasion assay indicated that the invasiveness of HeLa/Taxol cells was significantly greater than that of HeLa cells (Fig. 3C–D). Protein blot data of caspase apoptosis and waveform protein blot data of cell migration is shown in Supplementary Fig. 1A, column statistics are shown in Supplementary Fig. 1B, and statistical results are shown in Supplementary Table 1.

### 3.4. Detection of tumor stem cell markers in HeLa and HeLa/Taxol cells

Flow cytometry was employed to detect tumor stem cell markers including  $\text{CD44}^+$ ,  $\text{CD24}^+\text{CD44}^+$ , and  $\text{CD133}^+$  in both HeLa and HeLa/Taxol cells. The results indicated that the proportions of  $\text{CD24}^+$ ,  $\text{CD24}^+\text{CD44}^+$ , and  $\text{CD133}^+$  were all significantly higher in HeLa/Taxol cells compared to HeLa cells, suggesting an enrichment of stem cell-like features in the paclitaxel-resistant cell population (Fig. 4A–D).

### 3.5. Enhanced tumor stemness in HeLa/Taxol cells and identification of $\text{CD133}^+\text{ABCC5}^+$ as a potential tumor stem cell marker

In line with findings from previous studies [25,26], the expression levels of FOXM1 and ABCC5 were significantly elevated in HeLa/Taxol cell lines. To identify which markers most accurately represent tumor stem cells, additional flow cytometry assays were performed to assess the ratios of  $\text{ABCC5}^+$ ,  $\text{FOXM1}^+$ ,  $\text{CD24}^+\text{CD44}^+\text{ABCC5}^+$ ,  $\text{CD44}^+\text{ABCC5}^+$ ,  $\text{CD24}^+\text{CD44}^+\text{FOXM1}^+$ ,

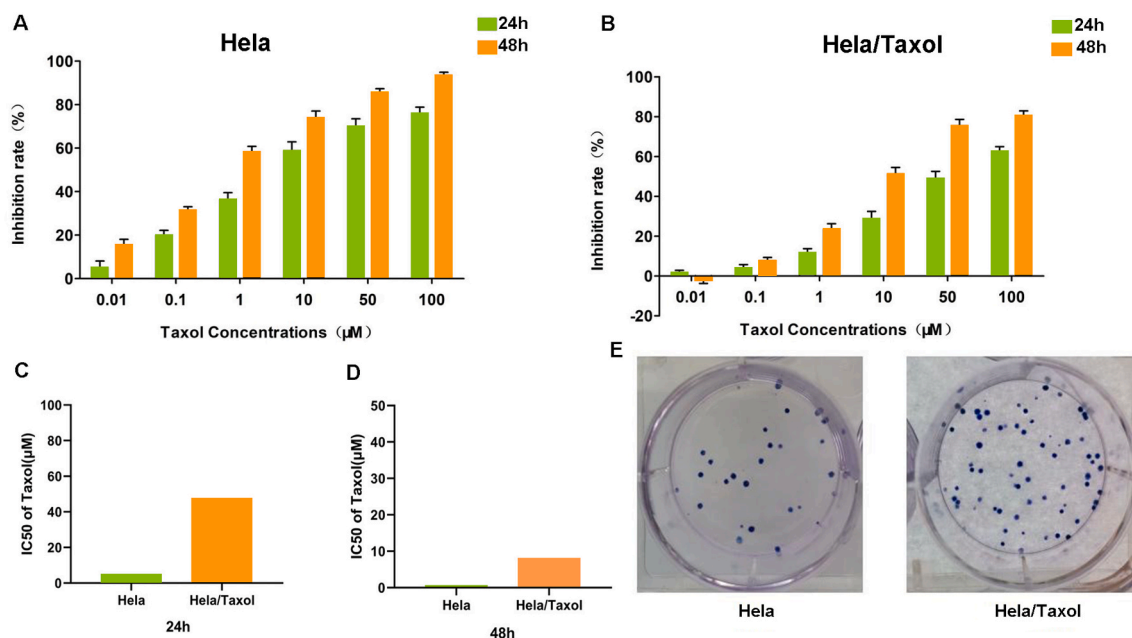


**Fig. 1.** Effects of different concentrations of paclitaxel on the proliferation of HeLa and HeLa/Taxol cells. (A) Histogram of HeLa cell proliferation. (B) Histogram of HeLa/Taxol cell proliferation. (C–D) IC50 histograms of HeLa and HeLa/Taxol cells. (E) Cell cloning of HeLa cells and HeLa/Taxol cells.

**Table 1**

Effects of different concentrations of paclitaxel on the proliferation of HeLa cells ( $\bar{x} \pm s$ , n = 5).

Drug Concentration (u M)	Inhibition rate (%)	
	24 h	48 h
0.01	5.034 ± 3.039	15.484 ± 2.600
0.1	19.934 ± 2.231 $\Delta$	31.407 ± 1.612 $\Delta$
1	36.396 ± 3.103 $\Delta$ $\blacktriangle$	58.237 ± 2.548 $\Delta$ $\blacktriangle$
10	58.763 ± 4.126 $\Delta$ $\nabla$	73.939 ± 3.099 $\Delta$ $\nabla$
50	69.977 ± 3.533 $\Delta$ $\nabla$ $\blacktriangledown$	85.462 ± 1.898 $\Delta$ $\nabla$ $\blacktriangledown$
100	75.893 ± 2.930 $\Delta$ $\nabla$ $\blacktriangledown$ $\star$	93.501 ± 1.363 $\Delta$ $\nabla$ $\blacktriangledown$ $\star$

Note:  $\Delta$  vs. 0.01  $\mu$ M, P < 0.01;  $\blacktriangle$  vs. 0.1  $\mu$ M, P < 0.01;  $\nabla$  vs. 1  $\mu$ M, P < 0.01;  $\blacktriangledown$  vs. 10  $\mu$ M, P < 0.01;  $\star$  vs. 100  $\mu$ M, P < 0.01.

**Table 2**

Effects of different concentrations of paclitaxel on the proliferation of HeLa/Taxol cells ( $\bar{x} \pm s$ , n = 5).

Drug Concentration (u M)	Inhibition rate (%)	
	24 h	48 h
0.01	1.641 ± 1.152	-2.083 ± 1.647
0.1	3.386 ± 1.849	7.707 ± 1.537 $\Delta$
1	11.546 ± 2.135 $\Delta$ $\blacktriangle$	23.551 ± 2.669 $\Delta$ $\blacktriangle$
10	28.740 ± 3.713 $\Delta$ $\nabla$	51.255 ± 3.259 $\Delta$ $\nabla$
50	48.933 ± 3.575 $\Delta$ $\nabla$ $\blacktriangledown$	75.508 ± 3.107 $\Delta$ $\nabla$ $\blacktriangledown$
100	62.521 ± 2.373 $\Delta$ $\nabla$ $\blacktriangledown$ $\star$	80.589 ± 2.272 $\Delta$ $\nabla$ $\blacktriangledown$ $\star$

Note:  $\Delta$  vs. 0.01  $\mu$ M, P < 0.01;  $\blacktriangle$  vs. 0.1  $\mu$ M, P < 0.01;  $\nabla$  vs. 1  $\mu$ M, P < 0.01;  $\blacktriangledown$  vs. 10  $\mu$ M, P < 0.01;  $\star$  vs. 100  $\mu$ M, P < 0.01.

**Table 3**

IC50 values for different times of paclitaxel intervention in HeLa, HeLa/Taxol cells.

Intervention time	IC50( $\mu$ M)		Resistance Index
	HeLa	HeLa/Taxol	
24 h	4.849	47.675	9.832
48 h	0.568	8.070	14.208

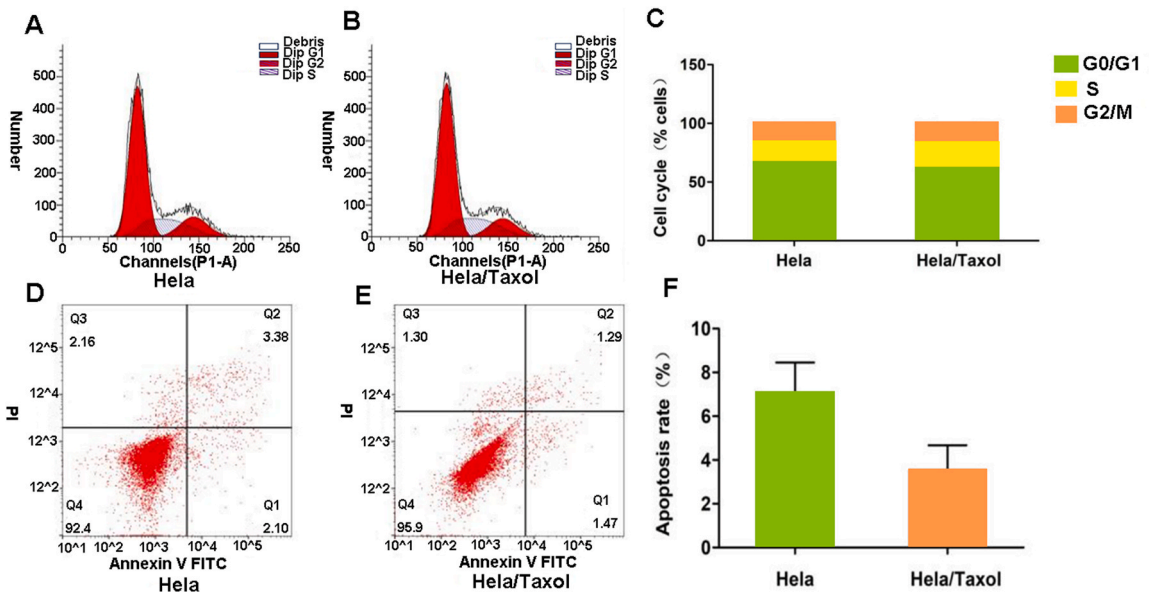


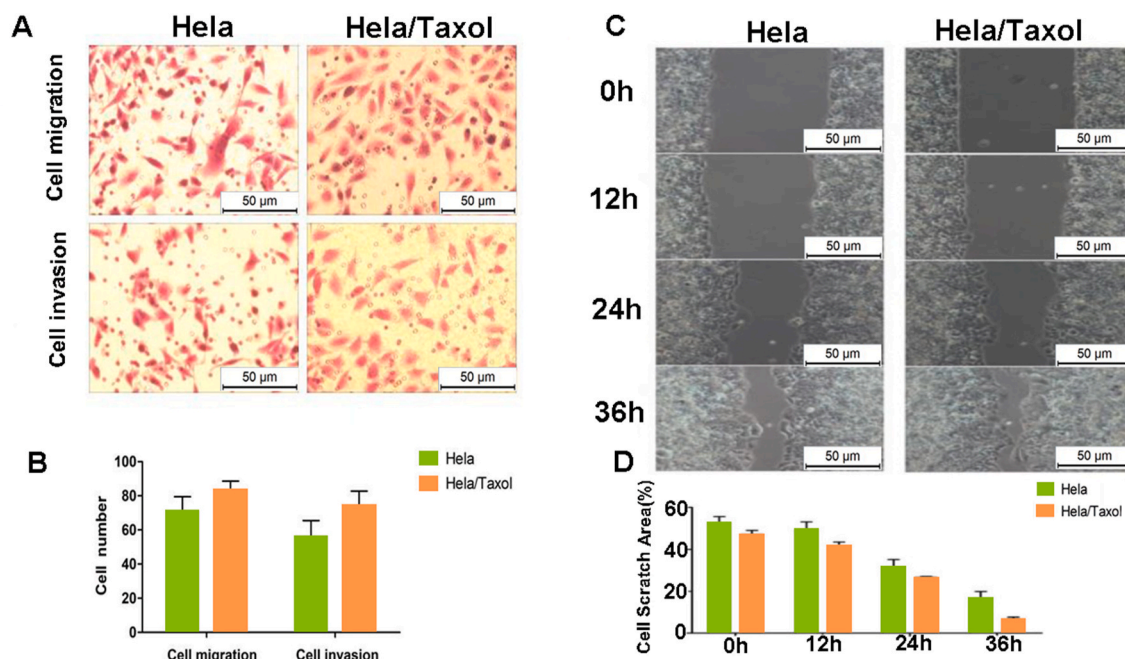
**Fig. 2.** HeLa cell and HeLa/Taxol cell cycle and apoptosis assays. (A–B) HeLa, HeLa/Taxol Flow Cycle Results Plot. (C) Comparative cell cycle profiles of HeLa and HeLa/Taxol cells. (D–F) HeLa, HeLa/Taxol apoptosis assay results.

**Table 4**Hela, Hela/Taxol cell cycle assay results( $\bar{x} \pm s$ , n = 3).

Experimental Grouping	G0/G1(%)	S (%)	G 2/M (%)
Hela	68.537 $\pm$ 0.236	17.777 $\pm$ 0.438	13.687 $\pm$ 0.437
Hela/Taxol	63.793 $\pm$ 0.386 $\Delta$	22.070 $\pm$ 0.632 $\Delta$	14.137 $\pm$ 0.726

Note:  $\Delta P < 0.01$  compared with Hela cells.**Table 5**Results of apoptosis detection in Hela, Hela/Taxol cells( $\bar{x} \pm s$ , n = 3).

Experimental Grouping	Apoptosis rate (%)
Hela	7.067 $\pm$ 1.385
Hela/Taxol	3.540 $\pm$ 1.133 $\Delta$

Note:  $\Delta P < 0.05$  compared with Hela cells.**Fig. 3.** Paclitaxel-resistant Hela cells exhibit increased migration and invasion. (A–B) Trans-well assay to observe the invasiveness of Hela and Hela/Taxol cell lines and their statistical bar graphs. (C–D) Migration rates of Hela and Hela/Taxol cells observed by scratch test and their bar charts.

CD44+FOXM1+, CD133+ABCC5+, and CD133+FOXM1+ cells. Excluding CD133+FOXM1+, all these cell ratios were significantly higher in Hela/Taxol cells compared to Hela cells (Fig. 5A–B). This indicates that Hela/Taxol cells are more prone to differentiate into tumor stem cells, suggesting a close association of FOXM1 and ABCC5 with tumor stem cell properties, potentially serving as new markers for these cells.

To further explore this hypothesis, CD133+ABCC5+ cells from both Hela and Hela/Taxol cells were isolated via flow cytometry sorting and cultured in stem cell medium for a stem cell spheroid assay. Results showed that both the size and number of spheroids formed by CD133+ABCC5+ cells from Hela/Taxol were significantly greater than those from Hela cells (Fig. 5C–D, Table 6), reinforcing the notion that Hela/Taxol cells exhibit greater tumor stemness. To substantiate these findings, Western blot analysis was performed to detect the expression of the stem cell-specific protein Sox2 and FOXM1 [26,27]. It was found that Sox2 and FOXM1 levels were significantly higher in CD133+ABCC5+ cells derived from Hela/Taxol compared to those from Hela cells (Fig. 5E–G, Table 7). This further confirms the enhanced tumor stemness of Hela/Taxol cells and supports the potential of CD133+ABCC5+ as a novel tumor stem cell marker.

#### 4. Discussions

Chemotherapy serves as a crucial treatment modality for cervical cancer, following surgery and radiotherapy, with paclitaxel



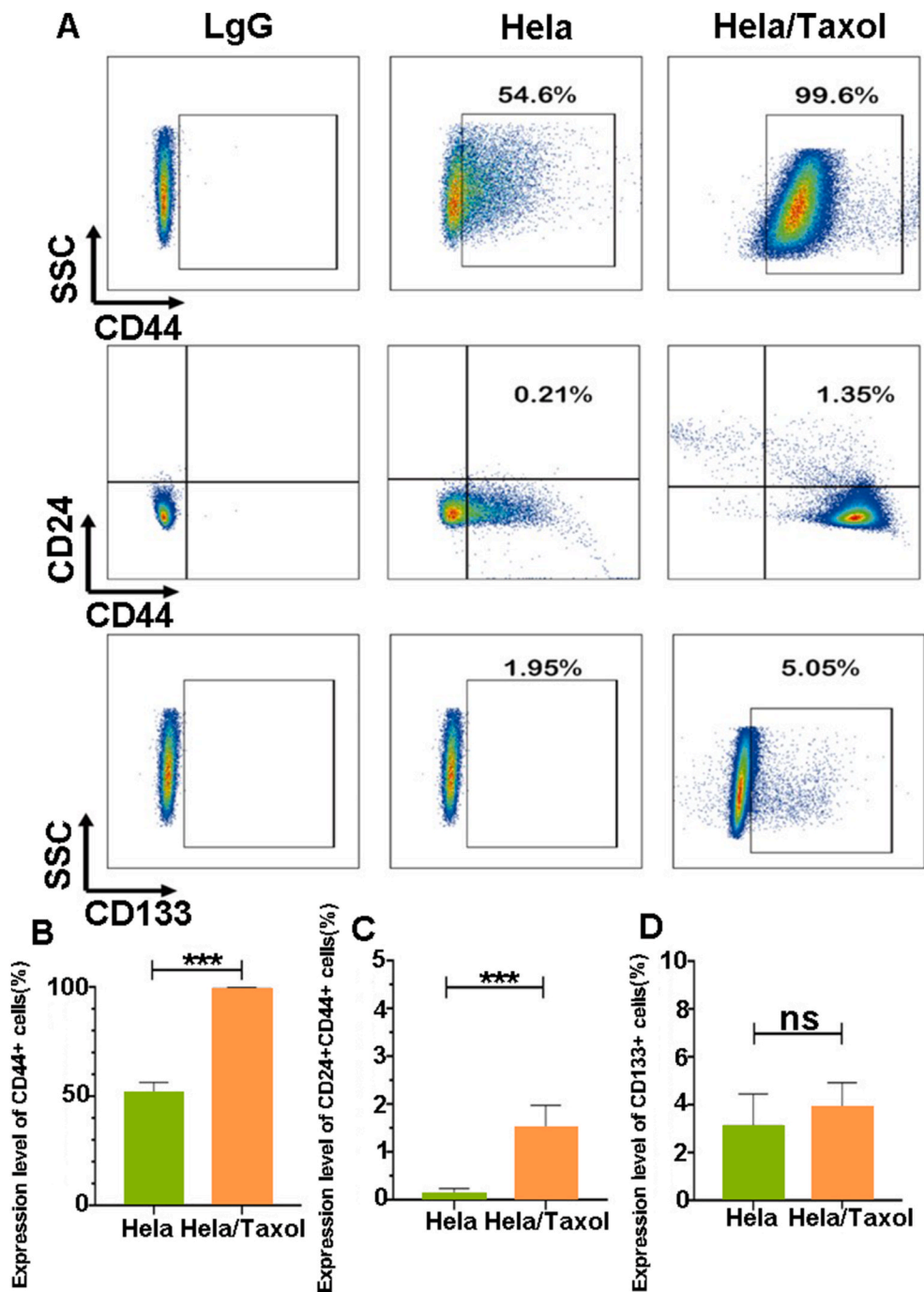


**Fig. 4.** Detection of tumor stem cells in HeLa versus HeLa/Taxol cells. (A) Flow assay of CD44<sup>+</sup>, CD24<sup>+</sup>CD44<sup>+</sup>, CD133<sup>+</sup> in HeLa and HeLa/Taxol cells. (B–D) Graph of CD44<sup>+</sup>, CD24<sup>+</sup>CD44<sup>+</sup>, CD133<sup>+</sup> statistics in HeLa and HeLa/Taxol cells.

combined with other drugs constituting the first-line chemotherapy regimen. However, the development of acquired resistance to paclitaxel significantly limits its clinical efficacy, resulting in a 20 %–30 % reduction in the 5-year survival rate of patients [28–30].

Resistance to paclitaxel involves a complex interplay of factors including the upregulation of ABC transporters, modifications in the microtubule system, dysregulation of non-coding RNA, activation of various signaling pathways, epithelial-mesenchymal transition (EMT), and alterations in autophagy and apoptosis mechanisms [31–36].

Recent studies have underscored the correlation between chemotherapy resistance and tumor stem cells [12,13]. In cervical cancer, specific markers for tumor stem cells remain undefined [18], highlighting the necessity to apply the concept of cancer stem cells (CSCs) to this cancer type. Actively identifying specific surface markers for cervical cancer CSCs could facilitate not only the sorting,

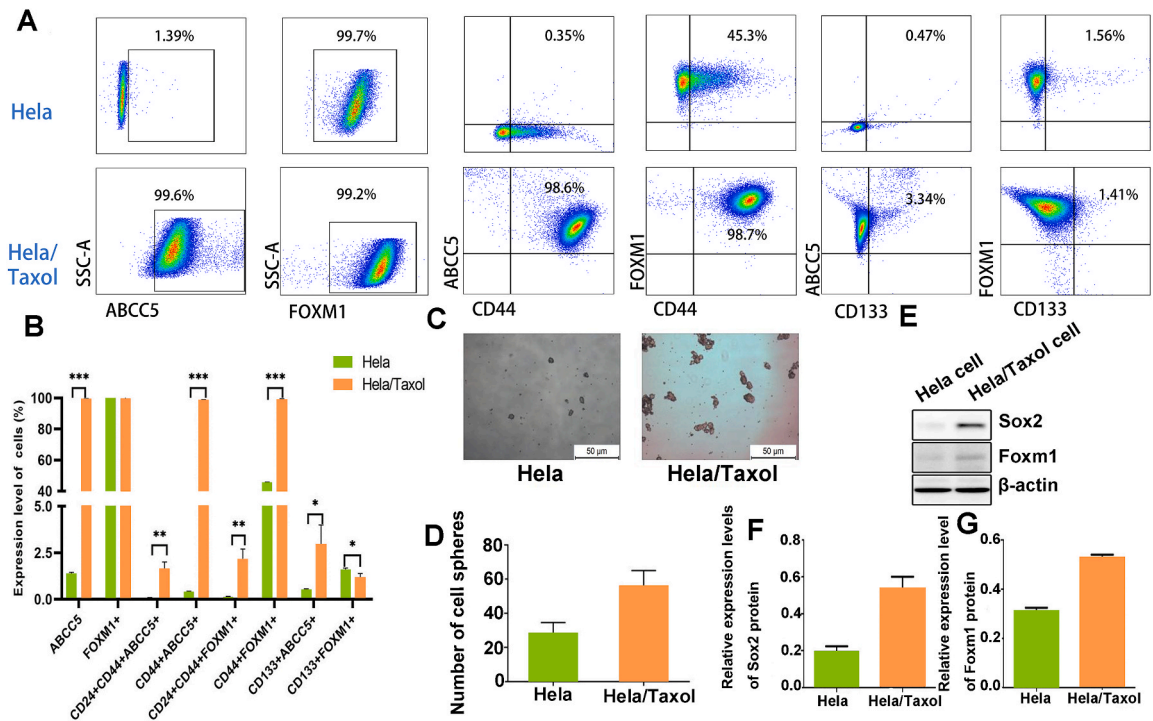


**Fig. 5.** HeLa/Taxol cells are more tumor stemness and CD133+ABCC5+ may be a new tumor stem cell marker. (A) Flow assay of ABCC5+, FOXM1+, CD24<sup>+</sup>CD44+ABCC5+, CD44+ABCC5+, CD24<sup>+</sup>CD44+FOXM1+, CD44+FOXM1+, CD133+ABCC5+, and CD133+FOXM1+ in HeLa and HeLa/Taxol cells and their statistical plots. (C–D) Sorted cell stem cell spheroid formation assay and statistical bar graph of HeLa, HeLa/Taxol cells. (E–F) Expression levels of Sox2 and FOXM1 proteins in CD133+ABCC5+ cells sorted from HeLa or HeLa/Taxol cells and bar graphs. The data are expressed as mean standard deviation (SD). \*P < 0.05, \*\*P < 0.01, \*\*\*P < 0.001.

**Table 6**  
Sorted cell stem cell spheroid formation results of HeLa, HeLa/Taxol cells( $\bar{x} \pm s$ , n = 3).

Group	Number of cell spheres
HeLa	34.667 ± 7.506
HeLa/Taxol	55.667 ± 9.292

Note:  $\Delta P < 0.01$  compared with HeLa cells.

**Table 7**  
Expression level analysis of Sox2 and FOXM1 proteins in CD133+ABCC5+ cells sorted from HeLa or HeLa/Taxol cells( $\bar{x} \pm s$ , n = 3).

Groups	Sox2	FOXM1
HeLa sorted cells	0.193 ± 0.030	0.308 ± 0.017
HeLa/Taxol sorting cells	0.533 ± 0.067	0.526 ± 0.014
T	-8.004	-17.404
P	0.001	0.000

enrichment, and characterization of these cells but also enhance early diagnosis, prognostic evaluation, and targeted therapy in clinical settings. Although molecular testing alone is insufficient to fully characterize tumor stem cells, targeting CSC-specific markers presents a promising and feasible strategy for their identification. Potential markers for cervical cancer stem cells that have been identified include CD133, CD24/CD44, ALDH1, CD49f, and SOX2 [26].

FOXM1, a member of the fork-head box transcription factor family characterized by a conserved winged helix DNA binding domain [37], plays a pivotal role in cell cycle regulation at the G1/S and G2/M phases, cell division, chromosome stability, and apoptosis [38, 39]. Overexpression of FOXM1 has been observed in various tumors [40,41] where it contributes to cancer progression by stimulating migration, invasion, angiogenesis, stem cell self-renewal, and therapeutic resistance [21,22].

ABCC5, part of the ATP-binding cassette (ABC) transporter superfamily and also known as multidrug resistance-associated protein



5, functions as a cyclic nucleotide organic anion transporter. It is implicated in the efflux of various substances from cells, playing a significant role in oncogenesis [23]. Research focusing on ABCC5 has revealed its impact on the effectiveness of cancer chemotherapy due to its ability to function as a drug efflux pump, facilitating the transport of molecules across cellular membranes and contributing to resistance against anticancer drugs [24]. Hence, ABCC5 is identified as a critical ABC transporter molecule involved in the resistance mechanisms against paclitaxel [19].

In recent years, ABCG2, a member of the ABC transporter family, has been identified as a half-transporter protein linked with multidrug resistance and as a potential marker for tumor stem cell identification [42]. Furthermore, other ABC transporters such as the breast cancer resistance protein and multidrug resistance protein 1 have been demonstrated to play critical roles in chemotherapy resistance in cervical cancer cells [43,44]. Consequently, targeting ABC transporters presents a promising strategy for addressing chemoresistance in cervical cancer. Chen et al. [45] first reported that olaparib markedly enhances the cytotoxicity of conventional chemotherapeutic agents against drug-resistant cervical cancer cell lines by binding to the active site of ABC transporters and inhibiting their function. Previous studies have highlighted the pivotal role of the FOXM1-ABCC5 axis in paclitaxel resistance in nasopharyngeal carcinoma cells [19] and demonstrated that FOXM1 modulates drug efflux and paclitaxel resistance through the transcriptional regulation of ABCC5 in cervical cancer cells [20].

This study builds upon these findings by examining the biological properties of HeLa and HeLa/Taxol cells using a series of assays, including cell proliferation, clone formation, cell cycle analysis, apoptosis, scratch tests, and transwell assays. Observations that HeLa/Taxol cells exhibit enhanced proliferation and invasion capabilities underscore the possible involvement of tumor stem cells. These observations were further substantiated by flow cytometry, sorting, and Western blot assays targeting tumor stem cells.

The current study amalgamates previous research to demonstrate that HeLa/Taxol cells exhibit increased tumor stemness compared to HeLa cells and that ABCC5+CD133+ may serve as a potential marker for tumor stem cells in cervical cancer. To the knowledge of the authors, this is the first study to suggest that ABCC5+CD133+ could be a marker of tumor stemness in cervical cancer, offering a new therapeutic target for overcoming paclitaxel resistance.

Although potential markers for cervical cancer stem cells have been identified in this study, there are notable limitations. As previously mentioned, relying solely on the expression levels of markers to define tumor stem cells may not adequately capture their true functional capabilities, such as self-renewal and differentiation potentials. Additionally, the inherent genetic and phenotypic heterogeneity within tumors suggests that a single cellular experimental model may not fully represent the distribution and function of tumor stem cells across the entire tumor. Furthermore, the expression of tumor stem cell markers can vary at different stages of tumor development and across various microenvironments, which cellular experiments might not effectively capture due to their static nature. To address these challenges, future research will focus on studying cervical cancer stem cell markers in tissue samples and animal models, employing *in vivo* validation to better understand the dynamic behavior of these markers. This approach will also include the development of inhibitors that specifically target cervical cancer stem cell markers, aiming to provide a more targeted and effective therapeutic strategy.

In conclusion, findings indicate that drug-resistant cervical cancer cell lines possess enhanced stemness, and that ABCC5+CD133+ may serve as potential markers for cervical cancer stem cells, laying a foundation for future research into targeted therapies.

## Funding information

This study was supported by the Regional Science Fund Program of the National Natural Science Foundation of China (82260520) and the Regional Science Fund Program of the National Natural Science Foundation of China (81860528).

## Data availability statement

It not applicable.

## CRedit authorship contribution statement

**Lin He:** Writing – original draft. **Hengjun Qian:** Data curation. **Ayinuer seyiti:** Formal analysis. **Chengshaoxiong Yang:** Data curation. **Ning Shi:** Formal analysis. **Chen Chen:** Data curation. **Pingxu Zhang:** Data curation. **Youxiang Hou:** Conceptualization.

## Declaration of competing interest

The authors declare that they have no known competing financial interests or personal relationships that could have appeared to influence the work reported in this paper.

## Appendix A. Supplementary data

Supplementary data to this article can be found online at <https://doi.org/10.1016/j.heliyon.2024.e37066>.

## References

- [1] F. Bray, M. Laversanne, H. Sung, Global cancer statistics 2022: GLOBOCAN estimates of incidence and mortality worldwide for 36 cancers in 185 countries, *Ca - Cancer J. Clin.* 74 (3) (2024) 229–263.
- [2] H. Sung, J. Ferlay, R.L. Siegel, Global cancer statistics 2020: GLOBOCAN estimates of incidence and mortality worldwide for 36 cancers in 185 countries, *Ca - Cancer J. Clin.* 71 (3) (2021) 209–249.
- [3] M. Arbyn, E. Weiderpass, L. Bruni, Estimates of incidence and mortality of cervical cancer in 2018: a worldwide analysis, *Lancet Global Health* 8 (2) (2020) e191–e203.
- [4] R.L. Siegel, Miller KD, Wagle NS. **Cancer statistics, 2023**, *Ca - Cancer J. Clin.* 73 (1) (2023) 17–48.
- [5] W. Cao, H.D. Chen, Y.W. Yu, Changing profiles of cancer burden worldwide and in China: a secondary analysis of the global cancer statistics 2020, *Chin Med J (Engl)*. 134 (7) (2021) 783–791.
- [6] N.C. Kampan, M.T. Madondo, O.M. McNally, Paclitaxel and its evolving role in the management of ovarian cancer, *BioMed Res. Int.* 2015 (2015) 413076.
- [7] X. Hong, S.Li W. Li, Disruption of protein neddylation with MLN4924 attenuates paclitaxel-induced apoptosis and microtubule polymerization in ovarian cancer cells, *Biochem. Biophys. Res. Commun.* 508 (3) (2019) 986–990.
- [8] Y. Zhao, X. Mu, G. Du, Microtubule-stabilizing agents: new drug discovery and cancer therapy, *Pharmacol. Therapeut.* 16 (2) (2016) 134–143.
- [9] A. Deborah, Sanders, V. Michael, FOXM1 binds directly to non-consensus sequences in the human genome, *Genome Biol.* 16 (6) (2015) 130–153.
- [10] A. Deborah, S. Caryn, Dario B. **Genome-wide mapping of FOXM1 binding reveals co-binding with estrogen receptor alpha in breast cancer cells**, *Genome Biol.* 14 (1) (2013) 1–16.
- [11] Chunyan Gu, Ye Yang, FOXM1 is a therapeutic target for high-risk multiple myeloma, *Leukemia* 30 (4) (2016) 873–882.
- [12] N. Lytle, A. Barber, T. Reya, Stem cells fate in cancer growth, progression and therapy resistance, *Nat. Rev. Cancer* 18 (2018) 669–680.
- [13] S. Chopra, K. Deodhar, Pai V. **Cancer stem cells, CD44, and outcomes following chemoradiation in locally advanced cervical cancer: results from a prospective study**, *Int. J. Radiat. Oncol. Biol. Phys.* 103 (1) (2019) 161–168.
- [14] M.N. Fahmi, I.N. Hertapanndika, F. Kusuma, The prognostic value of cancer stem cell markers in cervical cancer: a systematic review and meta-analysis, *Asian Pac. J. Cancer Prev. APJCP* 22 (12) (2021) 4057–4065.
- [15] A. Kohyama, R. Yokoyama, D.F. Dibwe, Synthesis of guggulsterone derivatives as potential anti-austerity agents against PANC-1 human pancreatic cancer cells, *Bioorg. Med. Chem. Lett* (2020) 126964.
- [16] J. Lathia, H. Liu, D. Matei, The clinical impact of cancer stem cells, *Oncol.* 25 (2) (2020) 123–131.
- [17] J.C. Ho, P.K. Allen, P.R. Bhosale, Diffusion-weighted magnetic resonance imaging as a predictor of outcome in cervical cancer after chemoradiation, *Int. J. Radiat. Oncol. Biol. Phys.* 97 (3) (2017) 546–553.
- [18] J. Zhang, X. Chen, L. Bian, CD44+/CD24+-Expressing cervical cancer cells and radioresistant cervical cancer cells exhibit cancer stem cell characteristics, *Gynecol. Obstet. Invest.* 84 (2) (2019) 174–182.
- [19] Y. Hou, Q. Zhu, Z. Li, The FOXM1-ABCC5 axis contributes to paclitaxel resistance in nasopharyngeal carcinoma cells, *Cell Death Dis.* 8 (2017) e2659.
- [20] Y. Hou, Z. Dong, W. Zhong, FOXM1 promotes drug resistance in cervical cancer cells by regulating ABCC5 gene transcription, *BioMed Res. Int.* 2022 (2022) 3032590.
- [21] L. Gu, H. Liu, Forkhead box M1 transcription factor: a novel target for pulmonary arterial hypertension therapy, *World J. Pediatr* 16 (2) (2020) 113–119.
- [22] P. Dey, A. Wang, Y. Ziegler, Suppression of tumor growth, metastasis, and signaling pathways by reducing FOXM1 activity in triple negative breast cancer, *Cancers* 12 (9) (2020) 2677.
- [23] L. Zhang, P. Huang, C. Huang, Varied clinical significance of ATP-binding cassette C sub-family members for lung adenocarcinoma, *Medicine (Baltim.)* 100 (16) (2021) e25246.
- [24] G. Ji, S. He, C. Huang, Upregulation of ATP binding cassette subfamily C member 5 facilitates prostate cancer progression and enzalutamide resistance via the CDK1-mediated AR Ser81 phosphorylation pathway, *Int. J. Biol. Sci.* 17 (7) (2021) 1613–1628.
- [25] H.S. Quah, E.Y. Cao, L. Suteja, Single cell analysis in head and neck cancer reveals potential immune evasion mechanisms during early metastasis, *Nat. Commun.* 14 (1) (2023) 1680.
- [26] R. Di Fiore, S. Suleiman, R. Drago-Ferrante, Cancer stem cells and their possible implications in cervical cancer: a short review, *Int. J. Mol. Sci.* 23 (9) (2022) 5167.
- [27] S. Boumahdi, G. Driessens, G. Lapouge, SOX2 controls tumour initiation and cancer stem-cell functions in squamous-cell carcinoma, *Nature* 511 (2014), 246–50.
- [28] R. Kitagawa, N. Katsumata, T. Shibata, Paclitaxel plus carboplatin versus paclitaxel plus cisplatin in metastatic or recurrent cervical Cancer : The open-label randomized phase III trial JCOG0505, *J. Clin. Oncol.* 33 (19) (2015) 2129–2135.
- [29] S. Mabuchi, K. Morishige, T. Enomoto, Carboplatin and paclitaxel as an initial treatment in patients with stage IVb cervical cancer : a report of 7 cases and a review of the literature, *J Gynecol Oncol.* 21 (2) (2010) 93–96.
- [30] D.H. Moore, J.A. Blessing, R.P. McQuellon, Phase III study of cisplatin with or without paclitaxel in stage IVB , recurrent , or persistent squamous cell carcinoma of the cervix : a gynecologic oncology group study, *J. Clin. Oncol.* 22 (15) (2004) 3113–3119.
- [31] R.W. Robey, K.M. Pluchino, M.D. Hall, Revisiting the role of ABC transporters in multidrug-resistant cancer, *Nat. Rev. Cancer* 18 (7) (2018) 452–464.
- [32] X. Shi, X. Sun, Regulation of paclitaxel activity by microtubule-associated proteins in cancer chemotherapy, *Cancer Chemother. Pharmacol.* 80 (5) (2017) 909–917.
- [33] T. Jeon, M.J. Ko, Y.R. Seo, Silencing CDCA8 suppresses hepatocellular carcinoma growth and stemness via restoration of ATF3 tumor suppressor and inactivation of AKT/ $\beta$ catenin signaling, *Cancers* 13 (5) (2021) 1055.
- [34] X. Wang, H. Wang, J. Xu, Double-targeting CDCA8 and E2F1 inhibits the growth and migration of malignant glioma, *Cell Death Dis.* 12 (2) (2021) 146.
- [35] T. Sun, D. Zhang, Z. Wang, Inhibition of the notch signaling pathway overcomes resistance of cervical cancer cells to paclitaxel through retardation of the epithelial-mesenchymal transition process, *Environ. Toxicol.* 36 (9) (2021) 1758–1764.
- [36] Y. Wang, F. Shen, J. Zhou, Overexpression of ARH1 increases the sensitivity of cervical cancer cells to paclitaxel through inducing apoptosis and autophagy, *Drug Dev. Res.* 83 (1) (2022) 142–149.
- [37] Q. Qin, H. Chen, H. Xu, FoxM1 knockdown enhanced radiosensitivity of esophageal cancer by inducing apoptosis, *J. Cancer* 14 (3) (2023) 454–463.
- [38] A.L. Gartel, FOXM1 in cancer: interactions and vulnerabilities, *Cancer Res.* 77 (12) (2017) 3135–3139.
- [39] Y. Shibui, K. Kohashi, A. Tamaki, The forkhead box M1 (FOXM1) expression and antitumor effect of FOXM1 inhibition in malignant rhabdoid tumor, *J. Cancer Res. Clin. Oncol.* 147 (5) (2021) 1499–1518.
- [40] X. Zhu, K. Lu, L. Cao, FoxM1 is upregulated in osteosarcoma and inhibition of FoxM1 decreases osteosarcoma cell proliferation, migration, and invasion, *Cancer Manag. Res.* 12 (2020) 9857–9867.
- [41] C.J. Barger, C. Branick, L. Chee, Pan-cancer analyses reveal genomic features of FOXM1 overexpression in cancer, *Cancers* 11 (2) (2019) 251.
- [42] L. Salphati, E.G. Plise, G. Li, Expression and activity of the efflux transporters ABCB1, ABCC2 and ABCG2 in the human colorectal carcinoma cell line LS513, *Eur. J. Pharmaceut. Sci.* 37 (3–4) (2009) 463–468.
- [43] M. Murahari, K.V. Prakash, G.J. Peters, Acridone-pyrimidine hybrids-design , synthesis , cytotoxicity studies in resistant and sensitive cancer cells and molecular docking studies, *Eur. J. Med. Chem.* 139 (2017) 961–981.
- [44] R. Sun, B. Jiang, H. Qi, SOX4 contributes to the progression of cervical cancer and the resistance to the chemotherapeutic drug through ABCG2, *Cell Death Dis.* 6 (11) (2015) e1990.
- [45] Z. Chen, K. Ling, Y. Zhu, Rucaparib antagonize multidrug resistance in cervical cancer cells through blocking the function of ABC transporters, *Gene* 759 (2020) 145000.